

Investigation on utilizing laser speckle velocimetry to measure the velocities of nanoparticles in nanofluids

Ming Qian, Jun Liu, Ming-Sheng Yan, Zhong-Hua Shen, Jian Lu and Xiao-Wu Ni*

*Department of Applied Physics, Nanjing University of Science and Technology, Nanjing, 210094,
People's Republic of China
nxw@mail.njust.edu.cn*

Qiang Li, Yi-Min Xuan

*School of Power Engineering, Nanjing University of Science and Technology, Nanjing, 210094,
People's Republic of China*

Abstract: Laser speckle velocimetry (LSV) is presented to measure the velocities of nanoparticles in nanofluids and its feasibility is verified in this paper. An optical scattering model of a single nanoparticle is developed and numerical computations are done to simulate the formation of the speckles by the addition of the complex amplitudes of the scattering lights from multiple nanoparticles. Then relative experiments are done to form speckles when nanofluids are illuminated by a laser beam. The results of the experiments are in agreement with the numerical results, which verify the feasibility of utilizing LSV to measure the velocities of nanoparticles in nanofluids.

©2006 Optical Society of America

OCIS codes: (030.6140) Speckle, (120.7250) Velocimetry.

References and links

1. U. S. Choi, "Enhancing thermal conductivity of fluids with nanoparticles," ASME Fed. **231**, 99-103 (1995).
2. P. Vadasz, "Heat conduction in nanofluid suspensions," J. Heat Transfer. **128**, 465-477 (2006).
3. Y. M. Xuan and W. Roetzel, "Conceptions for heat transfer correlation of nanofluids," Int. J. Heat Mass Transfer. **43**, 3701-3707 (2000).
4. S. P. Jang and S. U. S. Choi, "Role of Brownian motion in the enhanced thermal conductivity of nanofluids," Appl. Phys. Lett. **84**, 4316-4318 (2004).
5. R. Prasher, P. Brattacharya and P. E. Phelan, "Thermal conductivity of nanoscale colloidal solutions (nanofluids)," Phys. Rev. Lett. **94**, 025901 (2005).
6. W. Evans, J. Fish and P. Keblinski, "Role of Brownian motion hydrodynamics on nanofluid thermal conductivity," Appl. Phys. Lett. **88**, 093116 (2006).
7. H. W. Tang, Y. Yang and Y. R. Xu, "Study of several key techniques in PIV system," in Optical Measurement and Nondestructive Testing: Techniques and Applications; F. Song, F. Chen, M. Y. Y. Hung, and H. M. Shang; eds., Proc. SPIE **4221**, 361-365 (2000).
8. L. GmbH and A. V. Ring, "Visualization and PIV measurement of high-speed flows and other phenomena with novel ultra-high-speed CCD camera," in 25th International Congress on High-Speed Photography and Photonics; C. Cavailler, G. P. Haddleton, M. Hugenschmidt, eds., Proc. SPIE **4948**, 671-676 (2003).
9. A. Algieri, S. Bova and C. D. Bartolo, "Experimental and numerical investigation on the effects of the seeding properties on LDA measurements," J. Fluid Eng-T ASME **127**, 514-522 (2005).
10. S. J. Muller, "Velocity measurements in complex flows of non-Newtonian fluids," Korea-Aust Rheo. J. **14**, 93-105 (2002).
11. M. Kowalczyk, "Laser speckle velocimetry," in Optical Velocimetry; M. Pluta, J. K. Jabczynski, M. Szyjer; eds., Proc. SPIE **2729**, 139-145 (1996).
12. M. Kowalczyk, "Speckle velocimetry of diffuse objects under illumination of a TEM₁₀ laser beam," in Optical Velocimetry, M. Pluta, J. K. Jabczynski, and M. Szyjer, eds., Proc. SPIE **2729**, 146-154 (1996).
13. J. D. Briers, "Time-varying laser speckle for measuring motion and flow," in Saratov Fall Meeting 2000: Coherent Optics of Ordered and Random Media, D. A. Zimnyakov, ed., Proc. SPIE **4242**, 25-39 (2001).

14. J. D. Briers, "Laser Doppler and time-varying speckle: a reconciliation," *J. Opt. Soc. Am. A* **13**, 345-350 (1996).
 15. R. J. Adrian and C. S. Yao, "Pulsed laser technique application to liquid and gaseous flows and the scattering power of seed materials," *Appl. Opt.* **24**, 44-52 (1985).
 16. E. J. McCartney, *Optics of the atmosphere - Scattering by molecules and particles* (John Wiley & Sons, Inc. 1976).
-

1. Introduction

The conception of nanofluid [1] was first proposed by Choi of Argonne National Lab of United States in 1995. A certain volume fraction of nanoparticles, which remarkably enhance the heat transfer [2] of the fluid, were added into a base fluid in a certain manner.

Nanoparticles keep moving irregularly in nanofluids because of the effects of several factors such as gravity, Brownian force, and friction force between the fluid and particles. The irregular movements [3-6] of nanoparticles are the key factors that cause the remarkable enhancement of heat transfer of the nanofluids, so it is significant to investigate the movements of the nanoparticles in nanofluids for understanding the enhancement mechanism.

Considering that there is great comparability between detecting the movements of nanoparticles in nanofluids and measuring the velocity distribution of flow field by seeding fluid with small particles, particle image velocimetry (PIV) [7,8], laser Doppler velocimetry (LDV) [9,10] and LSV [11-13] may be useful in our present study, which both seed transparent fluid with some visible particles of micron magnitudes.

However, the ultrafine size of nanoparticle makes it have strong absorption and extremely weak scattering of the visible light, therefore, image of a single nanoparticle can not directly be formed on the recording film. As a result, available PIV technique is not competent for measuring the velocities of nanoparticles in nanofluids.

J. David Briers [14] reveals that LDV and LSV are effectively identical. However, in spite of their equivalence, there are distinctions between the two techniques. LDV is a pointwise technique for measuring the local velocity in a flowing fluid. In LDV, the Doppler frequency shift of laser light that has been scattered by small particles moving with the fluid is measured, and it depends only on the velocity of the particle and the scattering geometry. In order to be adapted to LDV applications, seeding particles must scatter enough light to produce a good signal-to-noise ratio. Therefore, the diameter of the seeding particle is typically 0.1 to 10 μm . And there is no literature reveals that LDV can be utilized to measure the velocities of nanoparticles in nanofluids so far.

However, in LSV, velocity distribution of the flowing fluid is obtained by measuring the velocities of the speckles formed by the interference of the scattering lights from multiple particles in fluid. According to Adrian [15] and Yao's research, the main difference between LSV and PIV is the concentration of the seeding particles in fluid. When the concentration is low, the distances between particles are so long that the scattering lights can not interfere, therefore, separate particle images will be formed on the recording film, and this is particle image mode. However, when the concentration is high, the distances between particles are short enough to satisfy the spatial interference condition, and light intensity in space is redistributed and speckles are formed on the recording film because of the interference of the scattering lights, and this is speckle pattern mode. Therefore, as far as the volume fraction of nanoparticles is kept proper, the distances between nanoparticles are short enough to satisfy the spatial interference condition, and the scattering light from different nanoparticles will interfere and form speckles on the recording film.

To verify the feasibility of utilizing LSV to measure the velocities of nanoparticles in nanofluids, the optical scattering characteristics of a single nanoparticle are researched, and numerical computations are done to simulate the formation of the speckles by the addition of the complex amplitudes of the scattering lights from nanoparticles in nanofluids. An experimental setup is established to do some relative experiments, in which nanofluids are illuminated by a monochromatic parallel laser beam to form speckles. And the correlation

between the two consecutive speckle patterns recorded by high speed CCD camera is obtained. The results of the experiments are in agreement with the numerical results.

2. Scattering characteristic of a single nanoparticle

2.1 Electric dipole model for Rayleigh scattering

It is Rayleigh scattering that acts when a nanoparticle is illuminated by a laser beam whose wavelength is much bigger than the diameter of the nanoparticle, and it can be described with electromagnetic wave theory.

As shown in Fig. 1, the incident light which is linearly polarized in Y axis direction illuminates along the forward direction of Z axis, the atom at the origin of coordinates becomes a electric dipole that oscillates along Y axis under the effects of the incident light and sends out secondary electromagnetic waves around, and this is the electric dipole model for Rayleigh scattering.

The electric dipole moment [16] is written as

$$P(t) = \frac{e^2}{m} \frac{1}{\omega_0^2 - \omega^2} E_0 \exp(i\omega t). \quad (1)$$

where ω is the circle frequency of the incident light; ω_0 is the natural frequency of the dipole; e is the charge of electron respectively; m is the quality of the nanoparticle; E_0 is the amplitude of the incident light.

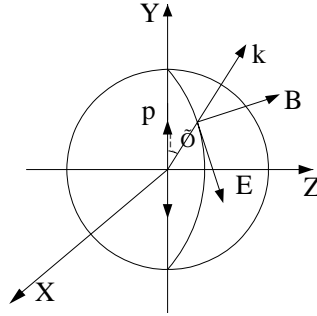


Fig. 1. Electric dipole model for Rayleigh scattering.

The electric-field intensity at a point that is R distant from the dipole is written as

$$\vec{E} = \frac{1}{4\pi\epsilon_0 c^2} \frac{[\ddot{\vec{p}}(t-R/c) \times \vec{R}] \times \vec{R}}{R^3}. \quad (2)$$

where the parameter $(t-R/c)$ represents the time delay; $\ddot{\vec{p}}$ is the second differential of the electric dipole moment and should be written as

$$\ddot{p}(t) = -\frac{e^2}{m} \frac{\omega^2}{\omega_0^2 - \omega^2} E_0 \exp(i\omega t). \quad (3)$$

Substituting Eq. (3) into Eq. (2) yields

$$\vec{E}_S = -\frac{\pi E_0}{\epsilon_0 \lambda^2} \frac{e^2}{m(\omega_0^2 - \omega^2)} \frac{\sin \phi}{R} \exp[i(\omega t - kR)] (\vec{p}_0 \times \vec{n} \times \vec{n}). \quad (4)$$

where ϕ is the angle between the propagating direction of the scattering light and the oscillating direction of the dipole; k is wave number and equals $2\pi/\lambda$; \vec{p}_0 is the oscillating direction of the incident light; \vec{n} is the direction vector of the scattering light and the subscript S denotes that \vec{E}_S is the electric-field intensity of the scattering light.

It can be concluded from Eq. (4) that the amplitude, phase and polarization of the scattering lights from the same nanoparticle at different points are different; and at the same

point in space, the amplitude, phase and polarization of the scattering lights from different nanoparticles are different too.

Considering the physical meaning of complex expression $\exp(i\alpha) = \cos \alpha + i \sin \alpha$, the complex amplitude of the scattering light can be written as

$$E_s = E_C \frac{\sin \phi}{R} \cos kR. \quad (5)$$

where E_C equals $-\frac{\pi E_0}{\epsilon_0 \lambda^2} \frac{e^2}{m(\omega_0^2 - \omega^2)}$.

2.2 Polarization of the scattering light

It can be concluded from above that, when a nanoparticle is illuminated by a monochromatic polarized light, the polarization of its Rayleigh scattering lights at different points in space are different.

Since the monochromatic laser beam used in our experiment is not polarized, it can be decomposed to two linearly polarized lights that oscillate along X axis and Y axis respectively. The intensity of the incident light is supposed to be I_0 , and each of the two linearly polarized lights has the intensity of $I_0/2$ and the amplitude of $\sqrt{2}E_0/2$.

When a nanoparticle is illuminated by a linearly polarized laser that oscillates along Y axis, its Rayleigh scattering light at a point on the screen is illustrated as Fig. 2. The nanoparticle locates at Point A whose coordinates are (x, y, z) , and its scattering light propagates to Point B whose coordinates are (x_1, y_1, z_1) . The coordinates of Point A' and C are respectively (x, y, z_1) and (x_1, y, z_1) . Plane ABC is parallel to Y axis. ϕ is the angle between the direction of the scattering light and the forward direction of Y axis, and it ranges from 0 to π . θ is the angle between plane ABC and plane YOZ .

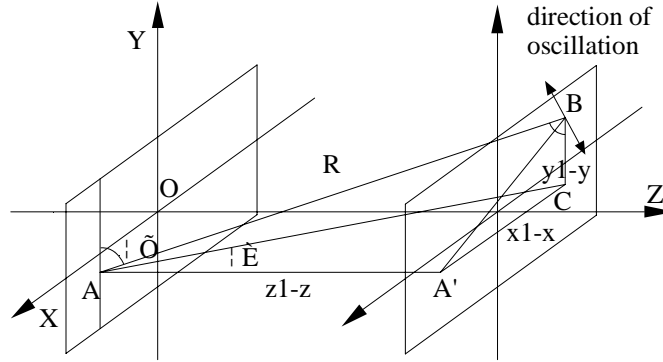


Fig. 2. Polarization of the scattering light when the incident light is Y axis polarized.

According to Fig. 2 the scattering light at Point B oscillates in plane ABC and is perpendicular to AB . $\cos \phi_Y = y_0/R$ and $\cos \theta_Y = z_0/(x_0^2 + z_0^2)^{1/2}$, where $x_0 = x_1 - x$, $y_0 = y_1 - y$, $z_0 = z_1 - z$ and the subscript Y denotes that the incident laser oscillates along Y axis. The complex amplitude of the scattering light at Point B can be decomposed respectively in the direction of X axis, Y axis and Z axis.

According to Eq. (5) and Fig. 2, the complex amplitude components can respectively be written as

$$E_x = E_s \cos \phi_Y \sin \theta_Y = \frac{\sqrt{2}}{2} E_C \cdot \frac{x_0 y_0}{R^3} \cdot \cos kR. \quad (6)$$

$$E_Y = E_S \sin \phi_Y = \frac{\sqrt{2}}{2} E_C \cdot \frac{x_0^2 + z_0^2}{R^3} \cdot \cos kR. \quad (7)$$

$$E_Z = E_S \cos \phi_Y \cos \theta_Y = \frac{\sqrt{2}}{2} E_C \cdot \frac{y_0 z_0}{R^3} \cos kR. \quad (8)$$

In like manner, as illustrated in Fig. 3, when a nanoparticle at Point A is illuminated by a linearly polarized laser that oscillates along X axis, its scattering light at Point B oscillates in plane ABC and is perpendicular to AB. $\cos \phi_X = x_0/R$ and $\cos \theta_X = z_0/(y_0^2 + z_0^2)^{1/2}$, where subscript X denotes that the incident laser oscillates along X axis. The complex amplitude of the scattering light at Point B can also be decomposed respectively in the direction of X axis, Y axis and Z axis and yields

$$E_X = E_S \sin \phi_X = \frac{\sqrt{2}}{2} E_C \cdot \frac{y_0^2 + z_0^2}{R^3} \cos kR. \quad (9)$$

$$E_Y = E_S \cos \phi_X \sin \theta_X = \frac{\sqrt{2}}{2} E_C \cdot \frac{x_0 y_0}{R^3} \cos kR. \quad (10)$$

$$E_Z = E_S \cos \phi_X \cos \theta_X = \frac{\sqrt{2}}{2} E_C \cdot \frac{x_0 z_0}{R^3} \cos kR. \quad (11)$$

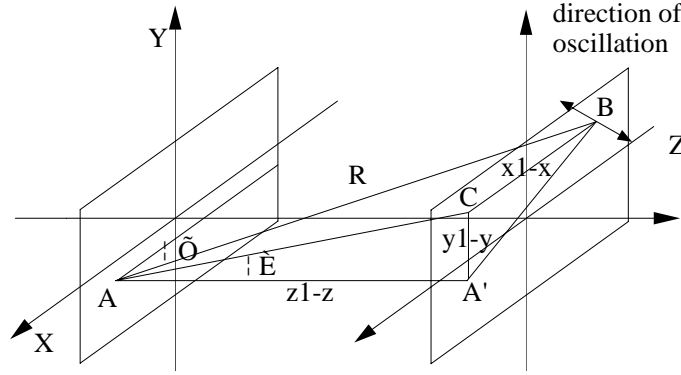


Fig. 3. Polarization of the scattering light when the incident light is X axis polarized.

Summing the corresponding Eqs. up yields

$$E_X = \frac{\sqrt{2}}{2} E_C \cdot \frac{x_0 y_0 + y_0^2 + z_0^2}{R^3} \cdot \cos kR. \quad (12)$$

$$E_Y = \frac{\sqrt{2}}{2} E_C \cdot \frac{x_0 y_0 + x_0^2 + z_0^2}{R^3} \cdot \cos kR. \quad (13)$$

$$E_Z = \frac{\sqrt{2}}{2} E_C \cdot \frac{x_0 z_0 + y_0 z_0}{R^3} \cdot \cos kR. \quad (14)$$

3. Speckle patterns formed by the scattering lights from multiple nanoparticles

When nanofluids are illuminated by a laser beam, speckles are formed by the addition of the complex amplitudes of the scattering lights from multiple nanoparticles. For any given nanoparticle whose coordinates are available, the complex amplitudes of the scattering light at any point in space should refer to Eqs. (12), (13) and (14). The total electric-field intensity at the point is

$$\vec{E} = \vec{i} \sum_{n=1}^{n=N} E_{nX} + \vec{j} \sum_{n=1}^{n=N} E_{nY} + \vec{k} \sum_{n=1}^{n=N} E_{nZ}. \quad (15)$$

where N is the number of the nanoparticles, E_{nx} , E_{ny} and E_{nz} are the complex amplitude components of the scattering light from the n th nanoparticle respectively in the direction of X axis, Y axis and Z axis.

3.1 Computational model

In order to do the numerical computations, a computational model is established as Fig. 4. The radius of the monochromatic parallel laser beam is 1mm. The screen is parallel to the back of the vessel and is 1cm distant. Nanoparticles are supposed to be approximately proportional spacing distributed in the vessel. The cylinder region that laser passes can be divided into plenty of little cubes. Each cube contains only one nanoparticle and the side length of the cube changes with the volume fraction of the nanoparticles. For example the side length is $0.94\mu\text{m}$ when the particle volume fraction is 0.0005%. By establishing this physical model the coordinates of each nanoparticle can be substituted with the central coordinates of the cube plus a random number which denotes the randomness of its coordinates. Therefore, the complex amplitude components of the scattering lights at any point on the screen from any nanoparticle can be obtained.

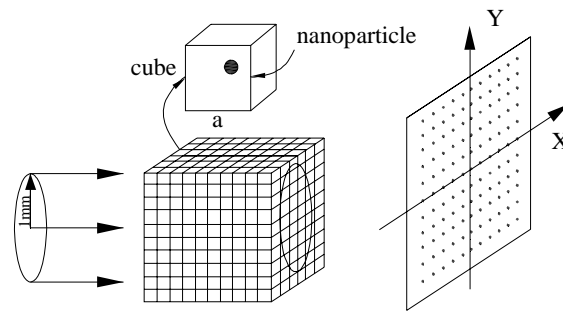


Fig. 4. Computational model.

3.2 Numerical results

On the basis of the computational model, numerical computations are done to simulate the formation of the speckles by the addition of the complex amplitudes of the scattering lights from nanoparticles. The complex amplitude components at any point refer to Eqs. (12), (13) and (14). As shown in Fig. 4, according to Eq. (15) the numerical computations are done at 121 points that even distributed on a $1\text{cm}\times 1\text{cm}$ square area in the center of the screen.

The intensities at the 121 points at two different moments are illustrated with bar charts in Fig. 5 while the thickness of the vessel is $10\mu\text{m}$. Several conclusions can be made as follow.

(1) The intensities at few points are much stronger than the intensities at the other points. Therefore, bright speckles are formed at few points.

More numerical computations are done while the thickness of the vessel ranges from $1\mu\text{m}$ to $100\mu\text{m}$, and the results show that the number of bright speckles occupies less than 9% of the total. Therefore, the speckle pattern formed on the screen or recorded by the CCD camera consists of relatively few bright speckles and plenty of dark speckles. It can also be concluded that the speckle pattern is in agreement with the normal distribution basically according to the numerical results.

(2) Comparing the two bar charts in Fig. 5, it is found out that there is great difference between them, which denotes that the intensity distribution of the speckle pattern on the screen changes with the movements of the nanoparticles, in other words, speckles move with the movements of the nanoparticles.

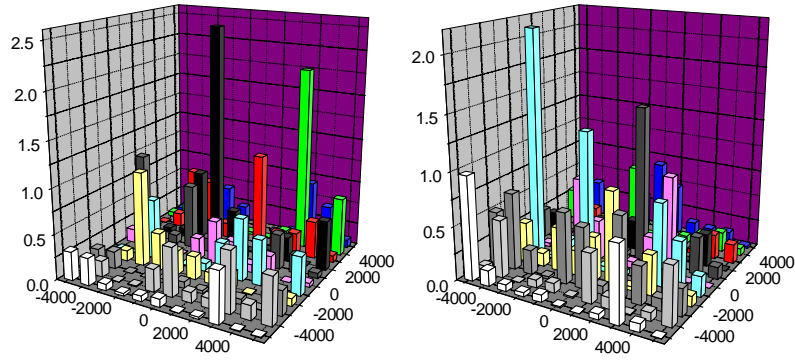


Fig. 5. Intensity distribution at two different moments when the thickness of the vessel is $10\mu\text{m}$.

3.3 Experimental results

Relative experiments are done to prove the results of the numerical simulations. The experimental setup is illustrated as Fig. 6. Nanofluids used in our experiment consist of water and a certain volume fraction of Fe_3O_4 nanoparticles whose average radius is 20nm . As shown in Fig. 6, a vessel filled with nanofluids is illuminated perpendicularly by a monochromatic parallel continuous laser beam with wavelength of 532nm and a screen or a high speed CCD camera is mounted parallel back of the vessel to observe or to record the speckles.

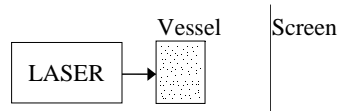


Fig. 6. Experimental setup.

Figure 7 is part of a typical speckle pattern recorded by high CCD camera while the power of the laser is 20mW , the thickness of the vessel is 1cm and the volume fraction of the nanoparticles is 0.0005% . The experimental results are in agreement with the numerical results basically.

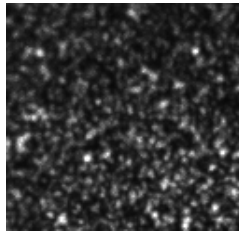


Fig. 7. Part of a typical speckle pattern.

3.4 Discussions

- (1) It can be concluded from Fig. 7 that the speckle pattern consists of relatively few bright speckles and plenty of dark speckles, which is in agreement with the numerical results.

This is because when a vessel filled with nanofluids containing a proper volume fraction of nanoparticles is illuminated perpendicularly by a monochromatic parallel laser beam, each nanoparticle will scatter light around. Since the scattering lights from different nanoparticles are all the secondary waves produced by the monochromatic incident laser, the time interference condition is satisfied; the distances between nanoparticles are small enough to satisfy the space interference condition, therefore, the scattering light will interfere on the screen and speckles are formed at few points bright. Numerical results also show that the speckles formed satisfy the normal distribution.

(2) It can also be found out in experiments that the bright speckles keep moving in the dynamic speckle pattern formed on the screen.

This is because at a given point on the screen, the amplitude, phase and polarization of the scattering light from each nanoparticle keep changing because of its random movement caused by the forces it suffers, so the intensity at that point keeps changing too. Consequently the movements of the nanoparticles cause the redistribution of the intensity on the screen, and the endless random movements of bright speckles can be seen clearly on the screen in experiment, which is verified by the numerical results too.

(3) In addition, it is found out that there is correlation between two consecutive speckle patterns recorded by high CCD camera.

The velocities of the speckles can be obtained by the cross-correlation calculation of the two patterns. The correlation between the movements of the nanoparticles and the movements of the speckles is discussed and obtained in another paper. Therefore, LSV can be utilized to measure the velocities of the nanoparticles in nanofluids.

4. Conclusion

An optical scattering model of a single nanoparticle is developed and the speckle patterns formed by the addition of the complex amplitudes of the scattering lights from multiple nanoparticles are numerically simulated. Experiments are done to verify the numerical results. It can be concluded from both the numerical and experimental results that speckles can be formed when nanofluids containing a certain volume fraction of nanoparticles are illuminated by a monochromatic laser beam. Since LSV utilizes the correlation between the movements of the seeding particles and the movements of the speckles formed by the interference of the scattering lights from the particles to measure the velocities of the particles, it can also be utilized to measure the velocities of the nanoparticles in nanofluids.

Acknowledgments

The work is supported by the National Natural Science Foundation of China, the Teaching and Research Award Program for Outstanding Young Professor in Higher Education Institute. MOE, P. R. China and the Specialized Research Fund for the Doctoral Program of Higher Education of China.